Complex stopover and migratory behavior revealed using mechanistic movement models with environmentally driven dynamic parameters

Joseph M. Eisaguirre[a,b,*], Marie Auger-Méthé[c,d], Christopher P. Barger[e], Stephen B. Lewis[f], Carol L. McIntyre[g], Travis L. Booms[e] and Greg A. Breed[a,h]

[a]Department of Biology & Wildlife, University of Alaska Fairbanks, Fairbanks, AK, USA

[b]Department of Mathematics & Statistics, University of Alaska Fairbanks, Fairbanks, AK, USA

[c]Department of Statistics, University of British Columbia, Vancouver, BC, Canada

[d]Institute for the Oceans & Fisheries, University of British Columbia, Vancouver, BC, Canada

[e]Alaska Department of Fish & Game, Fairbanks, AK, USA

[f]United States Fish & Wildlife Service, Juneau, AK, USA

[g]National Park Service, Fairbanks, AK, USA

[h]Institute of Arctic Biology, University of Alaska Fairbanks, Fairbanks, AK, USA

*Corresponding author: `jmeisaguirre@alaska.edu`

Author contributions: JME and GAB conceived the ideas of the research presented herein. JME, MA-M, and GAB designed analytical methods, and TLB, CPB, CLM, and SBL designed the field methodology. TLB, CPB, CLM, SBL, and JME collected the data. JME analyzed the data, and led the manuscript. All authors contributed to drafts and editing of the manuscript and provided final approval for publication.

Abstract

Long distance migration can increase lifetime fitness, but it can be costly, incurring increased energetic expenses and higher mortality risks. Stopover and other en route behaviors allow animals to rest and replenish energy stores and avoid or mitigate other hazards during migration. Some animals, such as soaring birds, can subsidize the energetic costs of migration with meteorological phenomena. However, it is unclear how these energy sources affect or interact with behavioral processes and stopover in long-distance soaring migrants. We used satellite telemetry to track a large soaring and opportunist foraging bird, the golden eagle *Aquila chrysaetos*, during migration in western North America and developed a flexible mechanistic model to predict how flight subsidies drive migrant behavior and movement processes. The model used time-varying parameters informed by environmental covariates to characterize a continuous range of behaviors during migration. We found a clear circadian rhythm in eagle movement and behavior, which was directly related to thermal uplift. Stopover behavior was complex, with evidence for a joint migrating/foraging behavior, resembling fly-and-forage migration, which could facilitate efficient refueling while still ensuring migration progress. Ecological and foraging conditions are normally considered to be key aspects of stopover location quality, yet opportunistic taxa, such as the golden eagle, may stopover based on both foraging opportunities and meteorology, permitting simultaneous search for food and flight subsidies.

Keywords

Bayesian, correlated random walk, golden eagle, movement ecology, soaring flight

Introduction

Long-distance migration can relax competition and permit use of seasonally available resources, helping many animals maximize lifetime fitness (Newton, 2008; Avgar et al., 2014). Those benefits, however, come at substantial costs, including greater vulnerability to predators, uncertain conditions, mechanical wear, elevated energy expenditure, and time (Alerstam and Hedenström, 1998; Clark and Butler, 1999; Hedenström, 2008; Newton, 2008; Avgar et al., 2014). As many migrant species cannot store sufficient energy for nonstop, long-distance migration, stopover evolved as a behavior for strategically resting and refueling en route (Gill, 2007).

Migrant species have wing morphologies adapted for utilizing either soaring or flapping flight, and the different morphologies relate to stopover strategy (Hedenström, 1993; Gill, 2007). Generally, soaring flight is favorable for larger birds and flapping flight for smaller birds, though the partitioning of time for each flight mode on migration is dependent on the relative importance of time- and energy-minimization (Hedenström, 1993; Duerr et al., 2015; Katzner et al., 2015). In theory, a bird minimizing migration duration (time minimizer) would be expected to fly with greater directional persistence and stronger directional bias relative to a bird minimizing energy expenditure. Such energy minimizers would be expected to respond more to local foraging cues and may divert or delay to take advantage of en route foraging opportunities. If time is less important, an energy-minimizer is less restricted and can spend additional time seeking an energetically superior path; the emergent path would then be more tortuous with less bias toward the final destination at any given point along the route.

Obligate soaring migrants must also consider routes based on their energy landscape (Shamoun-Baranes et al., 2010); the energetic constraints of movement over space (Shepard et al., 2013). While soaring migrants can stopover, their energy landscape is more complex; at least as important as foraging resources are meteorological conditions, which can be extremely dynamic and subsidize the energetic cost of flight directly via uplift (Pennycuick, 1971; Alerstam, 1979; Spaar and Bruderer, 1997; Gill, 2007; Duerr et al., 2012). Two primary forms of uplift arise by (1) the wind interacting with topography to

form upslope wind or mountain waves (air currents forming standing waves established on the lee side of mountains; hereafter orographic uplift) and (2) the sun heating the surface of the earth to generate thermal uplift. Other forms arise from turbulent eddies over small landscape features and ocean waves modifying the air. The flight performance of soaring migrants relative to meteorological conditions has been well documented (Pennycuick, 1971; Alerstam, 1979; Spaar and Bruderer, 1997), establishing a clear link between diurnal migrant behavior and development of the atmospheric boundary layer.

Global Positioning System (GPS) telemetry allows remote observation of animal relocations across a broad spatiotemporal scope. GPS transmitters are now light and reliable enough to study the complete migrations of many large soaring migrants, including golden eagles *Aquila chrysaetos*, which often rely on flight subsidies during migration (Katzner et al., 2015). Golden eagles and other large soaring birds have been used as model systems for phenomenologically evaluating questions about migratory flight performance and migration strategies (*sensu* Duerr et al., 2012; Lanzone et al., 2012; Katzner et al., 2015; Vansteelant et al., 2015; Miller et al., 2016; Shamoun-baranes et al., 2016; Rus et al., 2017). For example, Lanzone et al. (2012) and Katzner et al. (2015) found that golden eagles use both thermal and orographic uplift to subsidize migratory flight, although thermal soaring is often more efficient in long distance, directed flight (Duerr et al., 2012). These studies, however, relate meteorology to derived movement metrics, rather than the movement data themselves, and ignore the temporal dependence between serially observed locations, which can affect inference (Hooten et al., 2017). So, the mechanisms giving rise to behavioral budgets and stopover behavior during the migration of soaring birds remain unclear.

Process-based, mechanistic movement models allow explicit inference of the underlying mechanisms driving movement (e.g., changes in behavior) that may not be available from conventional phenomenological analytical approaches (Turchin, 1998; Nathan et al., 2008; Hooten et al., 2017). While it is impossible to fully understand the intricacies in animal movement, we can use mathematical models (e.g., correlated random walks) to approximate a movement process (Kareiva and Shigesada, 1983; Turchin, 1998), then use

statistics to fit the models to observed data and estimate process parameters (Morales et al., 2004; Hooten et al., 2017). Mandel et al. (2008) placed the migration of a soaring raptor in the framework of a movement model (i.e. a correlated random walk), yet reduced select components of movement (e.g., turning angles and distances) into separate statistical models in making inferences. Additionally, like the aforementioned studies, Mandel et al. (2008) did not address stopover behavior.

Here, we developed and applied a flexible mechanistic movement model based on a correlated random walk with time-varying parameters to movement data collected with GPS telemetry to address questions about how a population of long-distance soaring migrants uses flight subsidies to budget behavior. Specifically, we were interested in identifying which flight subsidies influence stopover and migratory behavior and how the effect of key subsides and behaviors might vary between spring and fall migration. Our approach resembled continuous-time correlated random walks (Johnson et al., 2008; Blackwell et al., 2015; Gurarie et al., 2017), yet was easily implemented and reduced to simple sets of biologically interpretable parameters and ranked models that indicated how behavioral budgets and meteorological variables interact to give rise to the observed migration paths.

Materials and methods

Model system

Golden eagles are a large soaring raptor distributed across the Holarctic (Watson, 2010). While many populations are classified as partial migrant, most individuals that summer and breed above approximately 55°N in North America are considered true long-distance migrants (Watson, 2010; Kochert et al., 2002). Golden eagles are predatory and opportunistic, utilizing many taxa for food resources, ranging from small mammals and birds to ungulates, often scavenging carrion (Kochert et al., 2002; Watson, 2010). Few movement data exist for adult golden eagles summering in Alaska and migrating across western North America, despite recent observations indicating that they likely occupy Alaska at

quite high summer densities (McIntyre and Schmidt, 2012; McIntyre and Lewis, 2016).

Data collection

We captured golden eagles with a remote-fired net launcher placed over carrion bait near Gunsight Mountain, Alaska (61.67°N 147.35°W). Captures occurred during spring migration, mid-March to mid-April 2014-2016. Adult and sub-adult eagles were equipped with 45-g back pack solar-powered Argos/GPS platform transmitter terminals (PTTs; Microwave Telemetry, Inc., Columbia, MD, USA). Eagles were sexed molecularly and aged by plumage.

PTTs were programmed to record GPS locations on duty cycles, ranging from 8-14 fixes per day during migration, depending on year of deployment. In 2014, PTTs were set to record 13 locations at one-hour intervals centered around solar noon plus a location at midnight local time. 2015 PTTs were programmed to record 8 locations with one-hour intervals centered around solar noon, and 2016 PTTs took eight fixes daily with a fixed 3-hr time interval. Poor battery voltage in fall, winter, and spring (September to March) often resulted in PTTs failing to take all programmed fixes, so the resulting GPS tracks had missing observations.

Movement data were managed in the online repository Movebank (`https://www.movebank.org/`), and we used the Track Annotation Service (Dodge et al., 2013) to gather flight subsidy (spatiotemporally explicit meteorological) data for each PTT location along eagle tracks. The Track Annotation Service derives uplift variables from elevation models and weather and atmospheric reanalyses (Bohrer et al., 2012). We followed the Movebank recommendations for interpolation methods; details are below.

Movement model

We developed a correlated random walk (CRW) movement model to reveal how changes in behavior give rise to the movement paths of migrating eagles. Behavioral models that use a discrete-state switching framework have proven powerful and useful for answering a variety of ecological questions (e.g., Morales et al., 2004; Jonsen et al., 2005; Breed et al.,

2009; Langrock et al., 2012). For this analysis, however, we chose to use a dynamic, time-varying correlation parameter, which represents behavior as a continuum rather than discrete categories, to capture complex behavioral patterns that could occur on multiple temporal and spatial scales (Breed et al., 2012; Auger-Méthé et al., 2017). We believe this approach is more inferential and computationally flexible, as a continuous range of behaviors is more realistic and, as we show, more naturally allows modeling behavior as a function of covariates.

The basic form of the model was a first-difference CRW presented by Auger-Méthé et al. (2017), which can take the form:

$$\mathbf{x}_i|\mathbf{x}_{i-1},\mathbf{x}_{i-2} \sim \mathcal{N}_2\left(\mathbf{x}_{i-1} + \gamma_i \frac{\Delta t_i}{\Delta t_{i-1}}(\mathbf{x}_{i-1} - \mathbf{x}_{i-2}),\ \mathbf{\Sigma}_i\right), \tag{1}$$

where

$$\mathbf{\Sigma}_i = \begin{bmatrix} \Delta t_i^2 \sigma_{lon}^2 & 0 \\ 0 & \Delta t_i^2 \sigma_{lat}^2 \end{bmatrix}, \quad \sigma_{lon}, \sigma_{lat} > 0. \tag{2}$$

Here, $\Delta t_i = t_i - t_{i-1}$ represents the time interval between Cartesian coordinate vectors $\mathbf{x}_i$ and $\mathbf{x}_{i-1}$ for the observed locations (or 'fixes') of the animal at times t_i and t_{i-1}, where $\mathbf{x}_i = \left(\begin{smallmatrix} longitude_i \\ latitude_i \end{smallmatrix}\right)$. We used the index i instead of t to reference observed locations because of the unequal time intervals (Auger-Méthé et al., 2017). Incorporating autocorrelation in behavior, γ_i was a random walk, such that

$$\gamma_i|\gamma_{i-1} \sim \mathcal{N}\left(\gamma_{i-1},\ \Delta t_i^2 \sigma_\nu^2\right), \quad \sigma_\nu > 0. \tag{3}$$

γ_i correlates displacements (or 'steps') and can be interpreted to understand the type of movement, and thus behavior, of migrating individuals: estimates of γ_i closer to one indicate directionally-persistent, larger-scale migratory movement, while estimates of γ_i closer to zero indicate more-tortuous, smaller-scale stopover movement (Breed et al., 2012; Auger-Méthé et al., 2017). Scaling γ_i by $\frac{\Delta t_i}{\Delta t_{i-1}}$ and the variance components by Δt_i^2 allows the model to accommodate unequal time intervals (Auger-Méthé et al., 2017), which can arise from a PTT's pre-programmed duty cycles and/or missed location attempts. This

assumes that over longer time intervals an animal is likely to move greater distances and that the previous step will have less influence on the current step. Notably, in introducing Δt_i, this CRW essentially becomes a correlated velocity model presented in terms of displacement vectors $(\mathbf{x}_{i-1} - \mathbf{x}_{i-2})$ (Johnson et al., 2008; Blackwell et al., 2015; Gurarie et al., 2017), most closely resembling the autocorrelated velocity model presented by Gurarie et al. (2017). This model does not consider spatial error in observations. Given the scale of movements and precision of GPS technology, we decided it unnecessary to incorporate an observation equation, which would have increased model complexity. Fixing covariance to zero (equation 2) assumes that movement in the x and y dimensions are independent, and although we made this assumption, covariance could easily be accounted for at the cost of increased model complexity.

Extending this CRW to introduce environmental covariates, we first made the assumption that an individual's behavior can be adequately explained by the previous behavior plus some effects of environmental conditions and random noise. This modeling approach and philosophy aligns with the movement ecology paradigm presented by Nathan et al. (2008): An animal's movement path is influenced by its internal state and the environmental conditions it experiences. We modified the behavioral (or internal state) process—previously described above as a pure random walk (equation 3)—similar to a linear model with a *logit* link function. The *logit* link constrains $\gamma_i \in [0, 1]$ and allowed us to model it as a linear combination of continuously-distributed random variables. These variables were different meteorological conditions affecting flight subsidies. Now,

$$\gamma_i = \frac{\exp\left(\gamma'_{i-1} + \mathbf{Z}_i\boldsymbol{\beta} + \epsilon_i\right)}{1 + \exp\left(\gamma'_{i-1} + \mathbf{Z}_i\boldsymbol{\beta} + \epsilon_i\right)}, \tag{4}$$

where

$$\gamma'_i = \log\left(\frac{\gamma_i}{1 - \gamma_i}\right), \tag{5}$$

$$\epsilon_i \sim \mathcal{N}\left(0,\ \Delta t_i^2 \sigma_\nu^2\right), \tag{6}$$

and $\mathbf{Z}_i$ is the design matrix of environmental covariates. Each element of $\boldsymbol{\beta}$ is an estimated parameter representing the magnitude and direction of the effect of its respective covariate

on the correlation parameter γ_i in addition to the effect of γ_{i-1}. Note that including γ_{i-1} here preserves explicit serial correlation in the behavioral process so that any additional environmental effect is not overestimated. γ_i' is only used to estimate γ_i; any behavioral interpretations are made in terms of γ_i.

Model fitting

Subsetting tracks

We fit the model to 15 spring and 16 fall adult (i.e. entering their fifth or later summer) golden eagle migration tracks recorded by 18 adult males and 8 adult females in 2016. Note that this included a repeated measure for five individuals; however, it was repeated for different seasons. In reporting the results, we assumed any effect of the few repeated measures to be negligible, which also seemed to be reasonable upon interpreting the results (Table S1). The model was fit to migration tracks plus two fixes prior to departure to ensure valid parameter estimates at the onset of migration. Data were subset to migration tracks under the following rules: The first migration step was identified as the first directed movement away from what was judged to be a seasonal home range with no subsequent return to that home range, and the final migration step was defined as the step terminating in the apparent opposing seasonal home range. This assignment was usually trivial; however, for some tracks there were apparent pre-migration staging areas, which were not considered part of migration.

Environmental covariates

Golden eagles can switch between using thermal and orographic uplift as flight subsidies (Lanzone et al., 2012; Katzner et al., 2015), so we included these variables as covariates affecting the correlation parameter in the behavioral process of the CRW (equation 4). Thermal uplift $\mathbf{z}_{tu}$ and orographic uplift $\mathbf{z}_{ou}$ are measured in m/s with $\mathbf{z}_{tu}, \mathbf{z}_{ou} \in [0, \infty)$. Thermal uplift was bilinearly interpolated from European Centre for Medium-Range Weather Forecasts (ECMWF) reanalyses, and orographic uplift from the nearest neighbor (grid cell) by pairing National Center for Environmental Predictions

(NCEP) North American Regional Reanalysis (NARR) data with the Advanced Spaceborne Thermal Emission Reflection Radiometer (ASTER) Global Digital Elevation Model (GDEM; Brandes and Ombalski, 2004; Bohrer et al., 2012). We also introduced wind as a covariate in the behavioral process, as it can influence eagle flight as well as the flight and energy landscape of many birds during migration (Shamoun-Baranes et al., 2017). Wind data were bilinearly interpolated from the NCEP NARR u (easterly/zonal) and v (northerly/meridional) components of wind predicted 30 m above ground, from which we calculated the tail wind support $\mathbf{z}_{tw}$, such that $\mathbf{z}_{tw} \in (-\infty, \infty)$ (Safi et al., 2013). The bearings used to calculate each $z_{tw,i}$ were the compass bearings required to arrive at $\mathbf{x}_{i+1}$ from $\mathbf{x}_i$.

We included a time of day interaction in the model because of clear diurnal effects. This also helped reduce zero inflation, particularly for thermal uplift, which often decays to zero after sunset due to heat flux and atmospheric boundary layer dynamics. To introduce the interaction, we used a dummy variable $\mathbf{z}_0$, such that $z_{0,i} = 0$ when t_i fell after sunset but before sunrise and $z_{0,i} = 1$ when t_i fell after sunrise but before sunset. This assumed behavior was not dependent on the covariates at night, which is sensible given observed diurnal behavioral cycles. Sunrise and sunset times local to each GPS point were calculated in R with the 'sunriset' function in the package 'maptools' (R Core Team, 2016; Bivand and Lewin-Koh, 2016). The final overall formulation of the behavioral process was:

$$\gamma'_i = \gamma'_{i-1} + [\beta_0 + \beta_{ou}(z_{ou,i} \times z_{0,i}) + \beta_{tu}(z_{tu,i} \times z_{0,i}) + \beta_{tw}(z_{tw,i} \times z_{0,i})] + \epsilon_i, \qquad (7)$$

Prior to fitting the model, we followed Gelman et al. (2008) and *log*-transformed the uplift covariates and standardized variance to 0.25. Rather than centering each uplift covariate distribution on zero, we used a shifted *log*-transformation; adding one to the covariates prior to the *log*-transformation preserved zeros (i.e. zeros mapped to zero under the transformation). The distribution of raw tail wind data appeared Gaussian, so it was only centered on zero and standardized.

Parameter estimation & model selection

We fit our CRW in a Bayesian framework. Because the model has explicit serially correlated parameters, we used Hamiltonian Monte Carlo (HMC) over more conventional Markov-chain Monte Carlo (MCMC; e.g., Gibbs sampling) to sample efficiently from a posterior with such correlation. Preliminary model testing indicated that HMC performed better; however, a formal comparison of MCMC algorithms is beyond the scope of this paper.

Gelman et al. (2008) suggested Cauchy priors for logistic regression parameters; however, Ghosh et al. (2015) found that sampling from the posterior can be inefficient due to the fat tails of the Cauchy distribution. We thus chose Student-t priors with five degrees of freedom as weakly informative priors for the covariate parameters. Concentrating the prior density on zero allowed convergence to nonzero coefficient estimates only when such were sufficiently supported by the data. Weakly informative normal priors were placed on the variance parameters of the model.

We implemented HMC with R and Stan through the package 'rstan' (R Core Team, 2016; Stan Development Team, 2016). Working R and Stan code, including details on prior choice, and example data are provided as electronic supplemental material, as well as supplementary tables and figures (Appendices 1-3). The model was fit to each track independently with five chains of 300,000 HMC iterations, including a 200,000 iteration warm-up phase, keeping every tenth sample. Convergence to the posterior distribution was checked with trace plots, effective sample sizes, posterior plots of parameters, and Gelman diagnostics ($\hat{R}$) for each model fit.

We compared candidate models with leave-one-out cross-validation approximated by Pareto-smoothed importance sampling (PSIS-LOO) in R with the package 'loo' (Vehtari et al., 2016, 2017). The candidate models included possible combinations of environmental covariates plus a null CRW model without covariates. To limit model complexity and because we were interested in competing hypotheses about key predictors of behavior, we chose not to include interactions beyond time-of-day. We ranked the models by the expected *log* pointwise predictive density (i.e. out-of-sample predictive accuracy)

transformed onto the deviance scale (looic; Vehtari et al., 2017), which allowed applying the rules of more traditional information-theoretic model selection (e.g., Burnham and Anderson, 2004). The model with the lowest looic was considered the best fit to the data, but if other models were within two looic of the top model, the top model was not considered a substantially better fit than those models.

Results

Model performance & diagnostics

Chain mixing, Gelman diagnostics ($\hat{R}$) close to one, and large effective sample sizes for all parameters indicated convergence to the posterior of our CRW model for most model fits. Posteriors of parameters appeared Gaussian, also indicating convergence (Fig. S1). For five migration tracks, we did not consider the null model converged to the posterior (e.g., $\hat{R} > 1.01$), while the full model still showed strong evidence for convergence. The few migrations with models that did not converge were excluded from formal model selection.

Behavior during migration

Median (interquartile range) departure and arrival dates were 5 March ($4.5\,d$) and 27 March ($6.4\,d$) in the spring and 29 September ($11.7\,d$) and 16 November ($15.5\,d$) in the fall. On average, eagles encountered similar orographic uplift in spring and fall but more intense thermal uplift and tailwind in the spring (Table 1).

The model revealed that eagles changed their behavior on multiple scales. First, there were very strong daily rhythms in behavior during migration, with birds moving and often migrating during the day and stopping at night (Figs. 1 & 2). While a time of day interaction explicitly in the model might drive a daily rhythm itself, accounting for serial correlation in behavior limits the overestimation of such an effect, as noted above and apparent in figure 2. Second, there was evidence for stopover behavior, though individuals tended to continue moving along their route when exhibiting stopover movements (Fig. 3). The continuation along the migration route while in a stopover-like state is highlighted

by track segments extended over space associated with low and intermediate estimates of γ_i (blue/purple in figure 3).

There was also a clear effect of season on movement patterns and behavior. Spring was characterized by straighter trajectories and punctuated stopovers; whereas, fall movements were much more tortuous and obvious regular patterns in stopover less clear (Figs. 1–3). The distributions of γ values also clearly indicate that daytime movements were most frequently migratory movements in the spring; whereas, in the fall, the bimodal distribution indicates more equivalent partitioning between migratory and stopover, with significant time spent exhibiting behaviors associated with intermediate tortuosity and displacement length (Fig. 3).

Environmental covariates

Including environmental covariates in the behavioral process generally improved model fit (Table 2). While there were differences in some environmental covariates between spring and fall (Table 1), parameter estimates from the full model (all covariates) indicate that there was little to no difference in effect of flight subsidies on behavior between spring and fall (Fig. 4, Table S1). Positive coefficients on the thermal uplift covariate indicate that increasing thermal uplift resulted in more highly-correlated displacements, or migratory movements. Despite that, there were some migration bouts not associated with great thermal uplift (Figs. 1 & 2). Coefficients close to zero for orographic uplift and tailwind indicate that they were not strong drivers of directionally-persistent movements.

Based on the model selection procedure, the best-fitting formulation of the behavioral process was variable among tracks and differed only slightly between seasons (Table 2). The substantial variability in best-fitting behavioral formulation among individual tracks (Table S1) was likely due to differing weather patterns and thus subsidy sources encountered and/or used by each animal as migrations were not synchronous across individuals. Consistent differences between sexes might be expected; however, some preliminary investigations did not reveal strong signals. We decided not pursue sex-specific effects in detail, in favor of focusing on seasonal patterns.

Discussion

We have shown how flight subsides give rise to a diversity in movement patterns within the long-distance migration of a soaring bird. Behavioral change occurs continuously as an animal moves through space and time and is a key mechanism underlying the emergent movement paths, yet this process is often hidden in our discrete observations of those paths. Our mechanistic modeling approach allowed linking meteorology to changes in behavior, and those changes in behavior to the observed migration paths, revealing time series of behaviors more complex than budgeting simply between migration and stopover.

Flight subsidies as drivers of behavior

Thermal uplift is a flight subsidy dependent on daily atmospheric boundary layer dynamics, and we found it to be a driver of the daily rhythm in eagle movements (Fig. 4, Table S1). Intense thermal uplift was often associated with the peaks of daily migration bouts (Fig. 1). The magnitude of the thermal uplift effect, relative to orographic uplift, was somewhat surprising, as many individuals in our sample followed the Rocky Mountains, which could be a source of orographic uplift. Golden eagles are known to use orographic uplift as a flight subsidy while migrating through the Appalachian Mountains in eastern North America (Katzner et al., 2015). Much of the Appalachians is characterized by long, unbroken, linearly-oriented ridges perfect for efficient use of predictable orographic uplift (Rus et al., 2017). This contrasts with the far more rugged, nonuniform, high-elevation Rocky Mountains, where conditions suitable for upslope winds and mountain waves, as well as strong tailwinds, likely generate violent turbulence and could impede efficient migratory flight. Soaring raptors have been shown to use small-scale turbulence to achieve subsidized flight (Allen et al., 1996; Mallon et al., 2016); however, unpredictable, non-stationary violent turbulence, which can occur in large, high-elevation mountain ranges (Ralph et al., 1997), would potentially correspond to energetically-demanding migration conditions for eagles. The large effect of thermal uplift, thus, could indicate that the Rocky Mountains, a spine that spans the migration nearly in its entirety, as well as some

areas further west, serve as thermal streets for migrating eagles (Pennycuick, 1998). More explicitly, intense sun on south facing slopes in the mountain ranges could generate linear series of thermals that birds could glide between during both spring and fall migration. It is important to keep in mind that the migrants could capitalize on fine-scale, localized features of certain flight subsidies, like orographic uplift and tailwind, that may not have been captured by the interpolated meteorological data used in our analyses. However, support for models with those variables in the model selection procedure do indicate they explained aspects of eagle movement, which is discussed further below.

Despite meteorological conditions along migration paths likely varying between spring and fall and a stark difference between behavioral budgets, our results showed no clear difference in effect of how flight subsidies drive behavioral dynamics between seasons (Fig. 4). This finding from our mechanistic approach contrasts with season-specific effects of flight subsidies on golden eagle migration shown phenomenologically in eastern North America, where primarily thermal uplift seemingly effects migratory performance in the spring and wind in addition to thermal uplift in the fall (Duerr et al., 2015; Rus et al., 2017). Nonetheless, our results suggest that the eagles can use similar flight subsidizing strategies to achieve quite different behavioral budgets: In the spring, time limitation drives use of subsidies to budget behavior in favor of migration progress such that they arrive on the breeding grounds as early as possible, and in the fall, subsidizing flight for behaviors favoring energy-minimization emerges as a much more diverse behavioral budget, composed of a more uniform range of movement patterns (Fig. 3; Miller et al., 2016). The punctuated stopovers in the spring (Fig. 3), however, suggest eagles pause and transition to another behavior to lower energy expenditure, refuel, and/or wait for better migration conditions. This aligns some with an energy-minimization strategy (Hedenström, 1993; Miller et al., 2016), despite the need for timely arrival on the breeding grounds to avoid fitness costs (Both and Visser, 2001).

The resulting behavioral time series showed some evidence of individuals responding less to thermal uplift as latitude increased during spring migration (Fig. 1). We also found a general decay in thermal uplift with increasing latitude during spring across indi-

viduals (Fig. S2). Reduced thermal uplift availability would be expected with increasing latitude due to the extent of remaining spring snowpack being greater at higher latitudes. Thus, golden eagles, and perhaps other soaring birds, migrating to high latitudes may need to budget behaviors carefully between time- and energy-minimization during spring migration in an effort to combat limited flight subsidy and thus greater energy expenditure further north.

While our results show that thermal uplift is important to eagle behavioral budgets, the model selection procedure indicated orographic uplift and tailwind had power in predicting eagle movements. Additionally, the variability in top models among tracks (Tables 2 & S1) is evidence for individual-level variability in flight-subsidizing strategy, and likely another contributing factor was that individuals encountered different subsidies en route and used what was available. Given that the orographic uplift and tailwind parameter estimates were often negative or close to zero (Fig. 4, Table S1), those covariates likely predicted the periods of more tortuous stopover behavior (i.e. γ_i closer to zero). Tailwind occurred in top models for more individuals in the fall (Tables 2 & S1), which is consistent with findings from others (McIntyre et al., 2008; Rus et al., 2017) and suggests it may be important during southbound migrations. The fact that the null model (without flight subsidies) fit so few tracks the best (Tables 2 & S1) is evidence that weather and flight subsidies are quite important to how golden eagles budget stopover behavior during migration.

Daily rhythm & complex stopover

The full formulation of the movement model revealed two clear, realistic behavioral patterns in the long-distance migrations of golden eagles. First, there was a daily rhythm in behavior where movement patterns resembling migratory movements (i.e. γ_i close to one) occurred most frequently around midday or early afternoon, then eagles stopped each night (Figs. 1 & 2). Mechanistic models of animal movement have revealed diel behavioral rhythms in other taxa (Jonsen et al., 2006). The basic aspects of daily rhythms in vertebrate behavior have hormone controls (Cassone, 1990), but the benefits can include

balancing migration progress and foraging bouts (Newton, 2008). Soaring migrants can also benefit from diel patterns in the atmosphere. That is, consistent with our results, diurnal soaring migrants express a general circadian behavioral rhythm, where flight performance and behavior can be strongly tied to thermal development of the planetary boundary layer (Kerlinger et al., 1985; Leshem and Yom-Tov, 1989; Spaar and Bruderer, 1996, 1997; Mateos-Rodríguez and Liechti, 2012).

The second behavioral pattern revealed by our model was a general stopover pattern, whereby eagles changed behavior for one to several days while en route (Figs. 1–3). These changes were consistent with searching movements (i.e. γ intermediate or close to zero), likely representing foraging behavior. In terms of soaring raptors, very few reports of movement patterns and behavior during stopovers have been published. Stopover segments have been previously identified by speed or some other metric calculated from tracks, then excluded from subsequent analyses (e.g., Vansteelant et al., 2015; Katzner et al., 2015); occasionally, authors noted apparent enhanced tortuosity but explored it no further (e.g., Vansteelant et al., 2017). On occasions where stopover behavior was considered, classifications based on stay duration and travel distance or speed with hard cutoffs between migrating and not migrating segments were used (Duerr et al., 2015; Chevallier et al., 2011; Katzner et al., 2012; Miller et al., 2016). In contrast, our modeling framework aligned with the movement ecology paradigm (Nathan et al., 2008); it used the observed data—GPS locations, rather than a derived metric—and a theoretical movement process to infer behavior from movement patterns along tracks on a spectrum ranging from stopped to rapid, directionally-persistent movement.

During periods of movement resembling stopover, eagles tended to continue along their migration route, albeit with reduced speed and directional persistence (Figs. 1–3). This pattern suggests a joint migration/opportunistic foraging behavior that resembles fly-and-forage migration (Strandberg and Alerstam, 2007; Åkesson et al., 2012; Klaassen et al., 2017), which is consistent with observations of en route hunting behavior by Dekker (1985). Such behavior could be used to maintain balance between time expenses and energy intake, as it allows simultaneous migration progress and foraging. Opportunism

in foraging would be a key character to the behavior, as that would relax the need for individuals to stopover in specific habitat patches—required by most taxa with less flexibility in food (Piersma, 2007)—and allow searching while making migration progress. Although species may be able to expand their trophic niche at stopover sites to increase efficiency in energy intake (Davis and Smith, 2001; Andrei et al., 2009), in order to permit near-continuous progress and foraging, individuals must be able to extend opportunism to resources available across habitats. Even some soaring migrants that can subsidize flight, might stopover due to limited flexibility in diet; prey specialists would need to forage in particular habitat where their prey are available. Fly-and-forage behavior expands the traditional notion of stopover behavior, whereby a bird migrates until resting and refueling is required, at which point it stops for a brief period in specific habitat suitable for efficient foraging (Gill, 2007; Newton, 2008).

The tendency for eagles to employ this joint fly-and-forage behavior was most apparent during fall migration. In contrast, spring migration was typically composed of much more punctuated stopover events, yet the stopovers were still extended over space (Fig. 3), indicating the birds might employ the joint behavior in spring as well. During spring, hibernating mammalian prey would be minimally available, leaving carrion, along with a few non-migratory and -hibernating species (e.g., ptarmigan *Lagopus* spp. and hare *Lepus* spp.), as major food sources, which could help explain the punctuated stopovers. Alternatively, individuals could have been slowed by poor weather conditions (Rus et al., 2017). Large ungulate carcasses would be extremely rewarding in terms of energy accumulation. The carrion we used successfully to capture eagles was in fact ungulate (e.g., moose *Alces alces*), indicating that the particular population we sampled uses carcasses as a food resource during migration. The bimodal distribution for the behavioral parameter γ in fall shows that eagles tended to budget daytime behaviors approximately equally between migratory and stopover movements (Fig. 3); the high frequency and range of intermediate values are evidence for a more complex dynamic—fly-and-forage—rather than eagles simply switching between discrete behavioral states. Such behavioral complexity might be biologically important, allowing eagles to arrive on home ranges in

better condition compared to the case where behavioral budgets do not permit as much foraging opportunity. In contrast to fall, daytime movements in the spring were typically larger-scale and directionally-persistent (Fig. 3), consistent with a time minimization strategy, where eagles need to partition time in favor of migration progress to ensure timely arrival on the breeding grounds (Hedenström, 1993; Alerstam, 2011; Miller et al., 2016).

Model performance

Incorporating time-varying parameters into movement models has been infrequently utilized (Breed et al., 2012; Auger-Méthé et al., 2017), yet we have provided a case study for its utility and advanced the approach. Modeling the serial correlation in movement as a function of environmental covariates (equation 4), allowed simultaneous inference of behavior and the effect of potential behavioral predictors from animal trajectories with regular and irregular duty cycles containing missing observations. The behavioral patterns we found would be more difficult to reveal with a state-switching movement model (e.g., Michelot et al., 2016) because each step would be forced into a behavioral state from a set of usually 2-3 discrete states. Moreover, although hidden-state models have been introduced that have more than five discrete states (e.g., McClintock et al., 2012), these states can require ancillary data streams (e.g., accelerometry) to discriminate and remain extremely difficult to employ and interpret in practice (Patterson et al., 2017; Pohle et al., 2017).

While our CRW model revealed the same patterns across duty cycles (Figs. 1 & 2), the most detail in daily behavioral rhythms was revealed in tracks with a fixed 3-hr time interval (lower panel in figure 2), as it provided data throughout the 24-hr day at regular intervals. The duty cycles also seemed to impact model fitting. HMC permitted Bayesian inference rather efficiently for our model, considering elevated correlation in the posterior of parameters due to the model formulation. Model fits typically took no more than a few hours, though tracks with much more than several hundred locations could take longer. Preliminary fitting of our model with Stan and Template Model Builder

(following Auger-Méthé et al. (2017)) suggested that Maximum Likelihood estimation tends to fail frequently when tag programming results in less or uneven temporal coverage of each day (e.g., our 2015 duty cycle), while Bayesian inference still provided realistic parameter estimates in most cases. Although the model presented herein and the model presented by Auger-Méthé et al. (2017) can make up for irregular time intervals between observations, they do have limitations. Breed et al. (2011) offers an in-depth discussion of tag programming and its effects on inference.

Implications & conclusions

We developed and applied a movement model to help reveal the mechanisms underlying the migration of a long-distance soaring migrant. We found that variation in flight subsidies give rise to changes in migrant behavior with thermal uplift seemingly most important. While these findings might be expected given previous phenomenological work (e.g., Duerr et al., 2012; Lanzone et al., 2012; Katzner et al., 2015; Vansteelant et al., 2015; Miller et al., 2016; Shamoun-baranes et al., 2016; Rus et al., 2017), we were able to show how meteorology is a mechanism driving changes in movement patterns and thus behavior. In the behavioral budgets of migrating golden eagles, we identified an expected daily rhythm, as well as periods of stopover, migration, and a behavior that would allow nearly simultaneous foraging and migration. In particular, we revealed new patterns in behavior during migration of long-distance soaring migrants and showed that it is not necessarily as simple as switching between migration and stopover.

Conflicts of interest

The authors declare that they have no conflict of interest.

Ethical approval

All applicable institutional and/or national guidelines for the care and use of animals were followed.

Acknowledgements

We thank M. Kohan, B. Robinson, T. & D. Hawkins and many others for support in the field and J. Liguori and N. Paprocki for help aging eagles. We also thank T. Avgar, P. Doak, T. Katzner, and K. Kielland for helpful comments on drafts of the manuscript. Funding was provided by the Alaska Department of Fish & Game (ADF&G) through the federal State Wildlife Grant Program, and the U.S. Fish & Wildlife Service (USFWS) provided PTTs and data. JME was supported by the Calvin J. Lensink Fund during part of the project. MA-M acknowledges the support of the Natural Sciences and Engineering Research Council of Canada. The findings and conclusions of this paper are those of the authors and do not necessarily represent the views of the USFWS.

References

Åkesson S, Klaassen R, Holmgren J, Fox JW, Hedenström A. 2012. Migration routes and strategies in a highly aerial migrant, the common swift Apus apus, revealed by light-level geolocators. *PLoS ONE* **7**: 1–9. doi: 10.1371/journal.pone.0041195.

Alerstam T. 1979. Optimal use of wind by migrating birds: combined drift and over-compensation. *Journal of Theoretical Biology* **79**: 341–353. doi: 10.1016/0022-5193(79)90351-5.

Alerstam T. 2011. Optimal bird migration revisited. *Journal of Ornithology* **152**: 5–23. doi: 10.1007/s10336-011-0694-1.

Alerstam T, Hedenström A. 1998. The development of bird migration theory. *Journal of Avian Biology* **29**: 343–369. doi: 10.2307/3677155.

Allen PE, Goodrich LJ, Bildstein KL. 1996. Within- and among-year effects of cold fronts on migrating raptors at Hawk Mountain, Pennsylvania, 1934-1991. *The Auk* **113**: 329–338.

Andrei AE, Smith LM, Haukos DA, Surles JG, Johnson WP. 2009. Foraging ecology

of migrant shorebirds in saline lakes of the Southern Great Plains. *Waterbirds* **32**: 138–148. doi: 10.1675/063.032.0117.

Auger-Méthé M, Albertsen CM, Jonsen ID, Derocher AE, Lidgard DC, Studholme KR, Bowen WD, Crossin GT, Mills Flemming J. 2017. Spatiotemporal modelling of marine movement data using Template Model Builder (TMB). *Marine Ecology Progress Series* **565**: 237–249. doi: 10.3354/meps12019.

Avgar T, Street G, Fryxell JM. 2014. On the adaptive benefits of mammal migration. *Canadian Journal of Zoology* **92**: 481–490. doi: 10.1139/cjz-2013-0076.

Bivand R, Lewin-Koh N. 2016. maptools: Tools for Reading and Handling Spatial Objects.
URL `https://cran.r-project.org/package=maptools`

Blackwell PG, Niu M, Lambert MS, Lapoint SD. 2015. Exact Bayesian inference for animal movement in continuous time. *Methods in Ecology and Evolution* **7**: 184–195. doi: 10.1111/2041-210X.12460.

Bohrer G, Brandes D, Mandel JT, Bildstein KL, Miller TA, Lanzone M, Katzner T, Maisonneuve C, Tremblay JA. 2012. Estimating updraft velocity components over large spatial scales: contrasting migration strategies of golden eagles and turkey vultures. *Ecology Letters* **15**: 96–103. doi: 10.1111/j.1461-0248.2011.01713.x.

Both C, Visser ME. 2001. Adjustment to climate change is constrained by arrival date in a long-distance migrant bird. *Nature* **411**: 296–298. doi: 10.1038/35077063.

Brandes D, Ombalski DW. 2004. Modeling raptor migration pathways using a fluid-flow analogy. *Journal of Raptor Research* **38**: 195–207.

Breed GA, Costa DP, Goebel ME, Robinson PW. 2011. Electronic tracking tag programming is critical to data collection for behavioral time-series analysis. *Ecosphere* **2**: 10. doi: 10.1890/ES10-00021.1.

Breed GA, Costa DP, Jonsen ID, Robinson PW, Mills-Flemming J. 2012. State-space methods for more completely capturing behavioral dynamics from animal tracks. *Ecological Modelling* **235-236**: 49–58. doi: 10.1016/j.ecolmodel.2012.03.021.

Breed GA, Jonson ID, Myers RA, Bowen WD, Leonard ML. 2009. Sex-specific, seasonal foraging tactics in adult gray seals (Halichoerus grypus) are revealed by behaviour discriminating state-space models. *Ecology* **90**: 3209–3221.

Burnham KP, Anderson R. 2004. Multimodel inference: understanding AIC and BIC in model selection. *Sociological Methods & Research* **33**: 261–304. doi: 10.1177/0049124104268644.

Cassone VM. 1990. Effects of melatonin on vertebrate circadian systems. *Trends in Neurosciences* **13**: 457–464.

Chevallier D, Le Maho Y, Brossault P, Baillon F, Massemin S. 2011. The use of stopover sites by Black Storks (Ciconia nigra) migrating between West Europe and West Africa as revealed by satellite telemetry. *Journal of Ornithology* **152**: 1–13. doi: 10.1007/s10336-010-0536-6.

Clark CW, Butler RW. 1999. Fitness components of avian migration: A dynamic model of Western Sandpiper migration. *Evolutionary Ecology Research* **1**: 443–453.

Davis CA, Smith LM. 2001. Foraging strategies and niche dynamics of coexisting shorebirds at stopover sites in the southern Great Plains. *The Auk* **118**: 484–495. doi: 10.2307/4089808.

Dekker D. 1985. Hunting behavior of golden eagles, Aquila chrysaetos, migrating in southwestern Alberta. *The Canadian Field-Naturalist* **99**: 383–385.

Dodge S, Bohrer G, Weinzierl R, Davidson SC, Kays R, Douglas D, Cruz S, Han J, Brandes D, Wikelski M. 2013. The environmental-data automated track annotation (Env-DATA) system: linking animal tracks with environmental data. *Movement Ecology* **1**: 3. doi: 10.1186/2051-3933-1-3.

Duerr AE, Miller Ta, Lanzone M, Brandes D, Cooper J, O'Malley K, Maisonneuve C, Tremblay J, Katzner T. 2012. Testing an emerging paradigm in migration ecology shows surprising differences in efficiency between flight modes. *PLoS ONE* **7**: e35548. doi: 10.1371/journal.pone.0035548.

Duerr AE, Miller TA, Lanzone M, Brandes D, Cooper J, O'Malley K, Maisonneuve C, Tremblay Ja, Katzner T. 2015. Flight response of slope-soaring birds to seasonal variation in thermal generation. *Functional Ecology* **29**: 779–790. doi: 10.1111/1365-2435.12381.

Gelman A, Jakulin A, Pittau MG, Su YS. 2008. A weakly informative default prior distribution for logistic and other regression models. *Annals of Applied Statistics* **2**: 1360–1383. doi: 10.1214/08-AOAS191.

Ghosh J, Li Y, Mitra R. 2015. On the use of Cauchy prior distributions for Bayesian logistic regression. *ArXiv* **1507.07170**.

Gill FB. 2007. *Ornithology*. New York: W. H. Freeman and Company, third edition.

Gurarie E, Fleming CH, Fagan WF, Laidre KL, Hernández-Pliego J, Ovaskainen O. 2017. Correlated velocity models as a fundamental unit of animal movement: Synthesis and applications. *Movement Ecology* **5**: 1–18. doi: 10.1186/s40462-017-0103-3.

Hedenström A. 1993. Migration by soaring or flapping flight in birds: The relative importance of energy cost and speed. *Philosophical Transactions of the Royal Society B: Biological Sciences* **342**: 353–361. doi: 10.1098/rstb.1993.0164.

Hedenström A. 2008. Adaptations to migration in birds: behavioural strategies, morphology and scaling effects. *Philosophical Transactions of the Royal Society B* **363**: 287–299. doi: 10.1098/rstb.2007.2140.

Hooten MB, Johnson DS, McClintock BT, Morales JM. 2017. *Animal movement: statistical models for telemetry data*. New York: CRC Press.

Johnson DS, London JM, Lea MA, Durban JW. 2008. Continuous-time correlated random walk model for animal telemetry data. *Ecology* **89**: 1208–1215. doi: 10.1890/10-1922.1.

Jonsen I, Flemming J, Myers R. 2005. Robust state – space modeling of animal movement data. *Ecology* **86**: 2874–2880.

Jonsen ID, Myers RA, James MC. 2006. Robust hierarchical state-space models reveal diel variation in travel rates of migrating leatherback turtles. *Journal of Animal Ecology* **75**: 1046–1057. doi: 10.1111/j.1365-2656.2006.01129.x.

Kareiva PM, Shigesada N. 1983. Analyzing insect movement as a correlated random walk. *Oecologia* **56**: 234–238.

Katzner TE, Brandes D, Miller T, Lanzone M, Maisonneuve C, Tremblay JA, Mulvihill R, Merovich GT. 2012. Topography drives migratory flight altitude of golden eagles: implications for on-shore wind energy development. *Journal of Applied Ecology* **49**: 1178–1186. doi: 10.1111/j.1365-2664.2012.02185.x.

Katzner TE, Turk PJ, Duerr AE, Miller TA, Lanzone MJ, Cooper JL, Brandes D, Tremblay JA, Lemaître J. 2015. Use of multiple modes of flight subsidy by a soaring terrestrial bird, the golden eagle Aquila chrysaetos, when on migration. *Journal of Royal Society Interface* **12**: 20150530. doi: 10.1098/rsif.2015.0530.

Kerlinger P, Bingman V, Able KP. 1985. Comparative flight behavior of migrating hawks studied with tracking radar during autumn in Central New York. *Canadian Journal of Zoology* **63**: 755–761. doi: 10.1139/z85-110.

Klaassen RH, Schlaich AE, Bouten W, Koks BJ. 2017. Migrating Montagu's harriers frequently interrupt daily flights in both Europe and Africa. *Journal of Avian Biology* **48**: 180–190. doi: 10.1111/jav.01362.

Kochert MN, Steenhof K, McIntyre CL, Craig EH. 2002. Golden Eagle (Aquila chrysaetos). In Poole A (ed.) *The Birds of North America*. Ithaca: Cornell Lab of Ornithology.

Langrock R, King R, Matthiopoulos J, Thomas L, Fortin D, Morales JM. 2012. Flexible and practical modeling of animal telemetry data: hidden Markov models and extensions. *Ecology* **93**: 2336–2342. doi: 10.1890/11-2241.1.

Lanzone MJ, Miller Ta, Turk P, Brandes D, Halverson C, Maisonneuve C, Tremblay J, Cooper J, O'Malley K, Brooks RP, Katzner T. 2012. Flight responses by a migratory soaring raptor to changing meteorological conditions. *Biology Letters* **8**: 710–713. doi: 10.1098/rsbl.2012.0359.

Leshem Y, Yom-Tov Y. 1989. The use of thermals by soaring migrants. *Ibis* **183**: 667–674.

Mallon JM, Bildstein KL, Katzner TE. 2016. In-flight turbulence benefits soaring birds. *The Auk* **133**: 79–85. doi: 10.1642/AUK-15-114.1.

Mandel JT, Bildstein KL, Bohrer G, Winkler DW. 2008. Movement ecology of migration in turkey vultures. *Proceedings of the National Academy of Sciences of the United States of America* **105**: 19102–19107. doi: 10.1073/pnas.0801789105.

Mateos-Rodríguez M, Liechti F. 2012. How do diurnal long-distance migrants select flight altitude in relation to wind? *Behavioral Ecology* **23**: 403–409. doi: 10.1093/beheco/arr204.

McClintock BT, King R, Thomas L, Matthiopoulos J, McConnell BJ, Morales JM. 2012. A general discrete-time modeling framework for animal movement using multistate random walks. *Ecological Monographs* **82**: 335–349. doi: 10.1890/11-0326.1.

McIntyre CL, Douglas DC, Collopy MW. 2008. Movements of Golden Eagles (Aquila chrysaetos) from Interior Alaska during their first year of independence. *The Auk* **125**: 214–224. doi: 10.1525/auk.2008.125.1.214.

McIntyre CL, Lewis SB. 2016. Observations of migrating Golden Eagles (Aquila chrysaetos) in Eastern Interior Alaska offer insights on population size and migration monitoring. *Journal of Raptor Research* **50**: 254–264.

McIntyre CL, Schmidt JH. 2012. Ecological and environmental correlates of territory occupancy and breeding performance of migratory Golden Eagles Aquila chrysaetos in interior Alaska. *Ibis* **154**: 124–135. doi: 10.1111/j.1474-919X.2011.01181.x.

Michelot T, Langrock R, Patterson TA. 2016. moveHMM: an R package for the statistical modelling of animal movement data using hidden Markov models. *Methods in Ecology and Evolution* **7**: 1308–1315. doi: 10.1111/2041-210X.12578.

Miller TA, Brooks RP, Lanzone MJ, Brandes D, Cooper J, Tremblay JA, Wilhelm JAY, Duerr A, Katzner TE. 2016. Limitations and mechanisms influencing the migratory performance of soaring birds. *Ibis* **158**: 116–134. doi: 10.1111/ibi.12331.

Morales JM, Haydon DT, Frair J, Holsinger KE, Fryxell JM. 2004. Extracting more out of relocation data: building movement models as mixtures of random walks. *Ecology* **85**: 2436–2445. doi: 10.1890/03-0269.

Nathan R, Getz WM, Revilla E, Holyoak M, Kadmon R, Saltz D, Smouse PE. 2008. A movement ecology paradigm for unifying organismal movement research. *Proceedings of the National Academy of Sciences* **105**: 19052–9. doi: 10.1073/pnas.0800375105.

Newton I. 2008. *The migration ecology of birds.* London: Academic Press.

Patterson TA, Parton A, Langrock R, Blackwell PG, Thomas L, King R. 2017. Statistical modelling of individual animal movement: an overview of key methods and a discussion of practical challenges. *AStA Advances in Statistical Analysis* **101**: 399–438. doi: 10.1007/s10182-017-0302-7.

Pennycuick C. 1998. Field observations of thermals and thermal streets, and the theory of cross-country soaring flight. *Journal of Avian Biology* **29**: 33–43. doi: 10.2307/3677338.

Pennycuick CJ. 1971. Soaring behavior and performance of some East African birds, observed from a motor-glider. *Ibis* **114**: 178–218.

Piersma T. 2007. Using the power of comparison to explain habitat use and migration strategies of shorebirds worldwide. *Journal of Ornithology* **148**: S45–S59. doi: 10.1007/s10336-007-0240-3.

Pohle J, Langrock R, van Beest FM, Schmidt NM. 2017. Selecting the number of states in hidden Markov models: pragmatic solutions illustrated using animal movement. *Journal of Agricultural, Biological, and Environmental Statistics* **22**: 270–293. doi: 10.1007/s13253-017-0283-8.

R Core Team. 2016. R: A language and environment for statistical computing. URL `https://cran.r-project.org/`

Ralph FM, Neiman PJ, Levinson D. 1997. Lidar observations of a breaking mountain wave associated with extreme turbulence. *Geophysical Research Letters* **24**: 663–666. doi: 10.1029/97GL00349.

Rus AI, Duerr AE, Miller TA, Belthoff JR, Katzner TE. 2017. Counterintuitive roles of experience and weather on migratory performance. *The Auk* **134**: 485–497. doi: 10.1642/AUK-16-147.1.

Safi K, Kranstauber B, Weinzierl R, Griffin L, Rees EC, Cabot D, Cruz S, Proaño C, Takekawa JY, Newman SH, Waldenström J, Bengtsson D, Kays R, Wikelski M, Bohrer G. 2013. Flying with the wind: scale dependency of speed and direction measurements in modelling wind support in avian flight. *Movement Ecology* **1**: 4. doi: 10.1186/2051-3933-1-4.

Shamoun-baranes J, Bouten W, Loon EEV, Meijer C, Camphuysen CJ, Shamoun-baranes J. 2016. Flap or soar? How a flight generalist responds to its aerial environment. *Philosophical Transactions of the Royal Society B* **371**: 20150395. doi: 10.1098/rstb.2015.0395.

Shamoun-Baranes J, Bouten W, Van Loon EE. 2010. Integrating meteorology into research on migration. *Integrative and Comparative Biology* **50**: 280–292. doi: 10.1093/icb/icq011.

Shamoun-Baranes J, Liechti F, Vansteelant WM. 2017. Atmospheric conditions create freeways, detours and tailbacks for migrating birds. *Journal of Comparative Physiology A: Neuroethology, Sensory, Neural, and Behavioral Physiology* **203**: 509–529. doi: 10.1007/s00359-017-1181-9.

Shepard ELC, Wilson RP, Rees WG, Grundy E, Lambertucci SA, Vosper SB. 2013. Energy landscapes shape animal movement ecology. *The American Naturalist* **182**: 298–312. doi: 10.1086/671257.

Spaar R, Bruderer B. 1996. Soaring migration of Steppe Eagles Aquila nipalensis in Southern Israel: flight behaviour under various wind and thermal conditions. *Journal of Avian Biology* **27**: 289–301. doi: 10.2307/3677260.

Spaar R, Bruderer B. 1997. Optimal flight behavior of soaring migrants: a case study of migrating steppe buzzards, Buteo buteo vulpinus. *Behavioral Ecology* **8**: 288–297. doi: 10.1093/beheco/8.3.288.

Stan Development Team. 2016. RStan: the R interface to Stan, Version 2.10.1. URL `http://mc-stan.org`

Strandberg R, Alerstam T. 2007. The strategy of fly-and-forage migration, illustrated for the osprey (Pandion haliaetus). *Behavioral Ecology and Sociobiology* **61**: 1865–1875. doi: 10.1007/s00265-007-0426-y.

Turchin P. 1998. *Quantitative analysis of movement: measuring and modeling population redistribution in animals and plants.* Sunderland, Massachusetts, USA: Sinauer Associates.

Vansteelant WMG, Bouten W, Klaassen RHG, Koks BJ, Schlaich AE, Diermen JV, Loon EEV. 2015. Regional and seasonal flight speeds of soaring migrants and the role of weather conditions at hourly and daily scales. *Journal of Avian Biology* **46**: 25–39. doi: 10.1111/jav.00457.

Vansteelant WMG, Shamoun-Baranes J, Mclaren J, van Diermen J, Bouten W. 2017. Soaring across continents: decision-making of a soaring migrant under changing atmospheric conditions along an entire flyway. *Journal of Avian Biology* **48**: 887–896. doi: 10.1111/jav.01298.

Vehtari A, Gelman A, Gabry J. 2016. loo: efficient leave-one-out cross-validation and WAIC for Bayesian models. R package version 1.0.0.

Vehtari A, Gelman A, Gabry J. 2017. Practical Bayesian model evaluation using leave-one-out cross-validation and WAIC. *Statistics and Computing* **27**: 1413–1432. doi: 10.1007/s11222-016-9696-4.

Watson J. 2010. *The Golden Eagle*. New Haven: Yale University Press, second edition.

Tables

Table 1: Summary statistics of flight subsidies encountered by migrating golden eagles that summer in Alaska. Variables were interpolated in space and time from weather reanalyses to eagle locations recorded by GPS telemetry. Units for all variables are m/s.

Season	**Orographic Uplift**	**Thermal Uplift**	**Tailwind**
	mean[a] (*s.d.*)	*mean* (*s.d.*)	*mean* (*s.d.*)
Spring	0.41 (0.71)	0.61 (0.48)	2.09 (3.06)
Fall	0.43 (0.71)	0.39 (0.34)	1.37 (3.45)

[a]grand mean across discrete GPS locations with individual migration tracks pooled

Table 2: Number of golden eagle migration tracks recorded by GPS transmitters that each candidate formulation of the behavioral process in the correlated random walk model fit the best, according to approximate leave-one-out cross-validation (Table S1).

Model	**looic Tally**[a]		
	spring	fall	total
full[b]	4	3	7
therm + twind	2	4	6
oro + therm	3	3	6
oro	3	3	6
therm	2	3	5
oro + twind	2	2	4
twind	0	3	3
null	1	1	2

[a]tally given to model with lowest information criterion (looic; Vehtari et al., 2016); if one or more models were within two looic of the top model, each was given a tally
[b]oro + therm + twind

Figure legends

Figure 1. Time series of behavior parameter γ from correlated random walk model with full behavioral process (orographic uplift, thermal uplift, and tailwind support as predictors) for two golden eagles during spring migration with PTTs reporting on different duty cycles. Upper panel is 13 hourly centered on solar noon plus one at midnight, and the lower panel is 8 hourly centered on solar noon. γ close to one reflect movements associated with migratory behavior, and γ close to zero stopover behavior. Points are times of observations, and lines are linear interpolations between points. Hue indicates intensity of thermal uplift, with yellow indicating greater and blue lower. Note the daily rhythm in behavior associated with intense thermal uplift, stopover periods of one or more days, and the intermediate periods suggesting fly-and-forage.

Figure 2. Time series of behavior parameter γ from correlated random walk model with full behavioral process (orographic uplift, thermal uplift, and tailwind support as predictors) for three golden eagles during fall migration with PTTs reporting on different duty cycles. Upper panel is 13 hourly centered on solar noon plus one at midnight, middle panel is 8 hourly centered on solar noon, and lower panel is fixed 3-hr interval. γ close to one reflect movements associated with migratory behavior, and γ close to zero stopover behavior. Points are times of observations, and lines are linear interpolations between points. Hue indicates intensity of thermal uplift, with yellow indicating greater thermal uplift and blue lower. Note the daily rhythm in behavior and extended stopovers as well as periods intermediate values suggesting fly-and-forage.

Figure 3. Golden eagle migration trajectories ($N = 15$ spring and $N = 16$ fall). Hue indicates value of behavioral parameter γ estimated with the correlated random walk model with full behavioral process, including orographic uplift, thermal uplift, and tailwind support as predictors. Insets show the relative frequencies of estimates of γ assigned to the displacements between observed daytime GPS locations. γ close to one reflect movements associated with migratory behavior, and γ close to zero stopover behavior. Daily

rhythms, revealed in figures 1 and 2, are not apparent here because the birds moved so little at night.

Figure 4. Point estimates of environmental covariate effect parameters (β_{ou}, β_{tu}, β_{tw}) on golden eagle behavior and movements during migration ($N = 15$ spring and $N = 16$ fall). Estimates are from the correlated random walk model with full behavioral process, including orographic uplift, thermal uplift, and tailwind support as predictors.

Figures

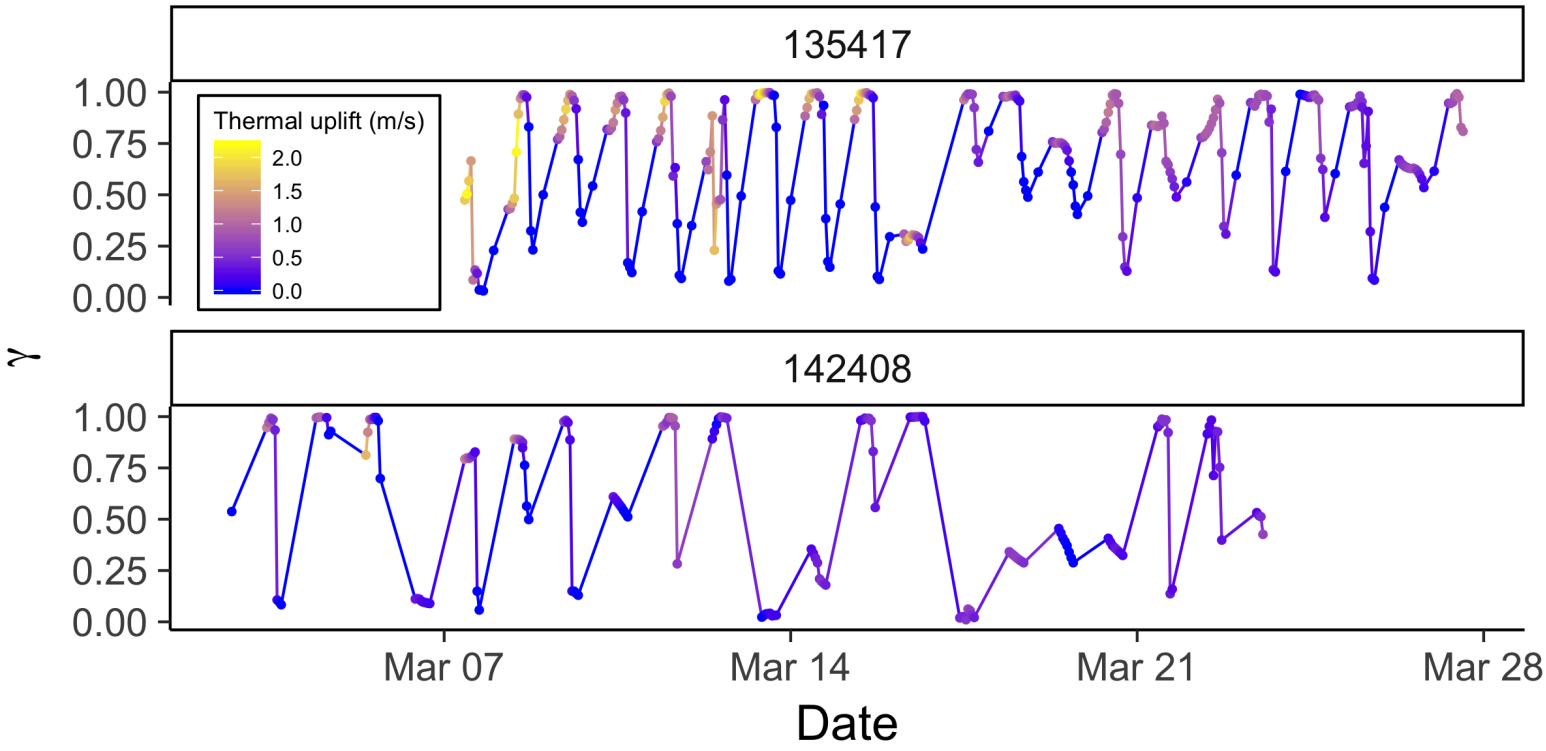

Figure 1

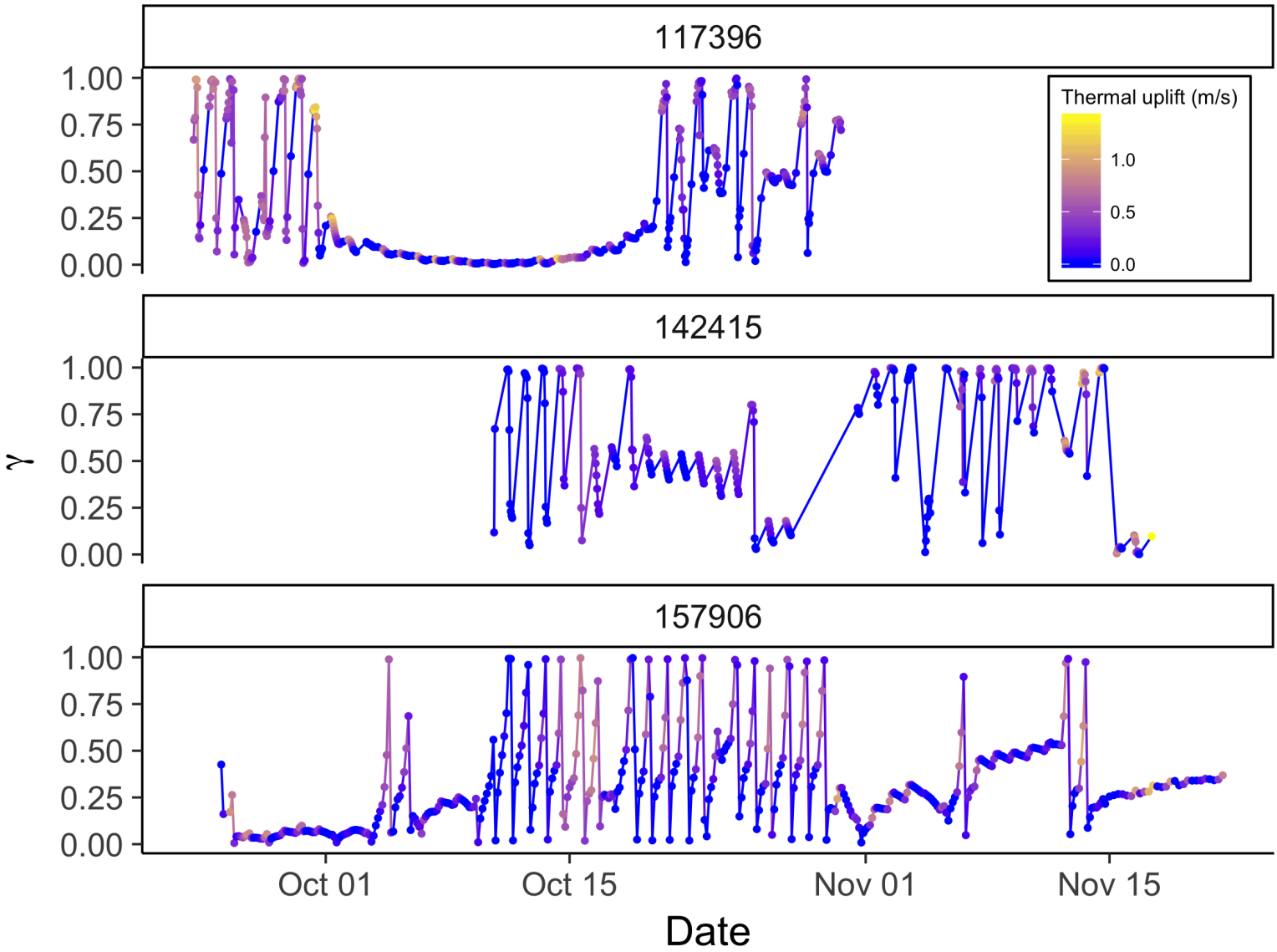
117396
142415
157906
1.00
0.75
0.50
0.25
0.00
γ
Thermal uplift (m/s)
1.0
0.5
0.0
Oct 01
Oct 15
Nov 01
Nov 15
Date

Figure 2

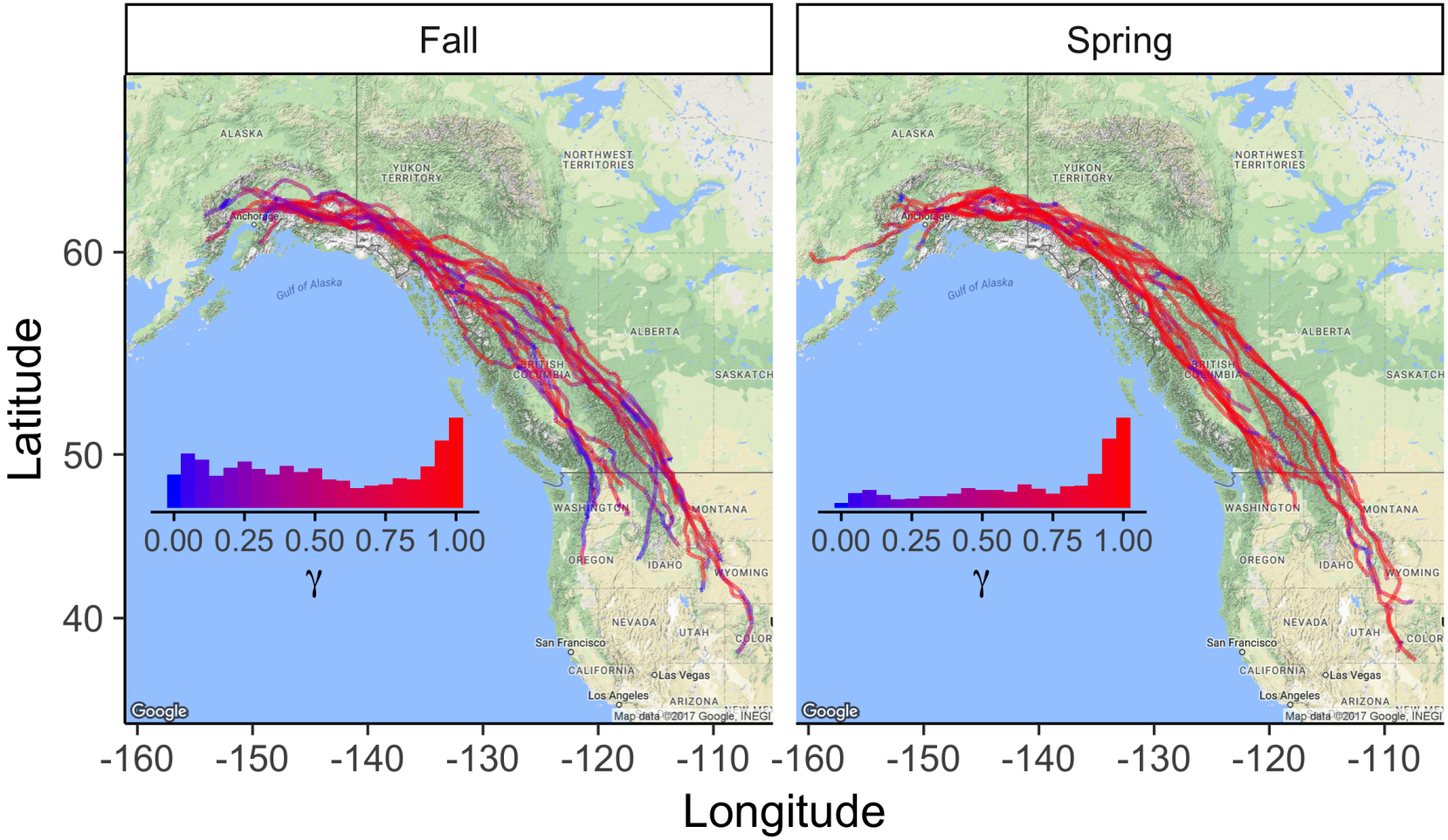
Fall
Spring
Latitude
60
50
40
0.00 0.25 0.50 0.75 1.00
γ
ALASKA
YUKON TERRITORY
NORTHWEST TERRITORIES
Anchorage
Gulf of Alaska
ALBERTA
SASKATCH
BRITISH COLUMBIA
WASHINGTON
MONTANA
OREGON
IDAHO
WYOMING
NEVADA
UTAH
San Francisco
CALIFORNIA
Las Vegas
Los Angeles
ARIZONA
Google
Map data ©2017 Google, INEGI
-160 -150 -140 -130 -120 -110
Longitude

Figure 3

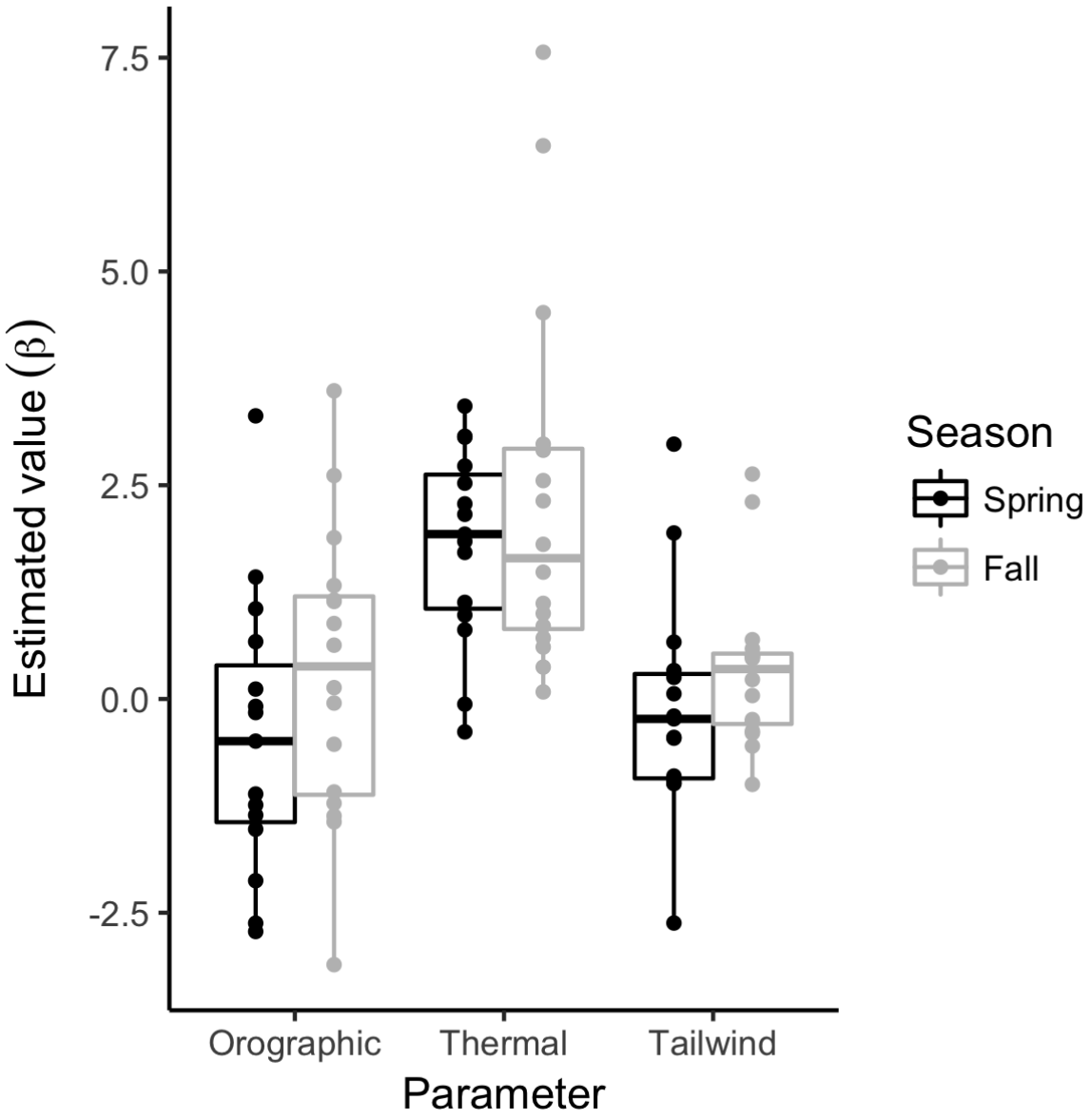
7.5
5.0
2.5
0.0
-2.5
Estimated value (β)
Orographic
Thermal
Tailwind
Parameter
Season
Spring
Fall

Figure 4

Appendix 1: supplementary tables & figures

Table S1: Estimates of environmental covariate effects on golden eagle behavior and movements during migrations. Parameter estimates are from the correlated random walk model with full behavioral process, including and intercept (β_0) orographic uplift (β_{ou}), thermal uplift (β_{tu}), and tailwind support (β_{tw}) as predictors. Top model is the best fitting candidate of the behavioral process resulting from an approximate leave-one-out cross-validation model selection procedure.

ID[a]	**Season**	**Parameter**[b]				**Top Model**[c]
		β_0	β_{ou}	β_{tu}	β_{tw}	
117394	spring	-2.68	-1.52	0.98	0.67	oro
117396	spring	-2.70	-0.49	3.07	-0.46	-
	fall	-0.53	-3.11	0.08	0.49	full[d] / oro + twind
117397	spring	-4.80	1.43	3.06	0.25	therm + twind / therm
117398	spring	-2.21	-0.09	0.81	-0.45	oro / therm
135411	spring	-2.55	-2.62	1.84	-0.98	oro + therm / full / oro + twind
135413	spring	-2.98	0.12	1.13	0.06	oro
135414	spring	-0.74	-1.11	-0.38	1.94	oro + twind
135417	spring	-2.53	-1.36	2.28	-0.20	oro + therm
	fall	-2.90	-0.53	0.85	2.30	therm
135421	fall	-2.78	-1.09	2.91	0.69	twind
135423	spring	-2.80	-1.24	2.52	-0.99	null
	fall	-2.12	0.13	1.00	-0.24	therm + twind
135425	fall	-2.29	-1.37	1.81	0.51	twind
142404	spring	-2.90	3.31	1.71	-2.62	full
142405	spring	2.34	1.06	1.93	-0.96	full / oro + therm
142407	spring	-2.11	-0.16	2.72	2.98	therm + twind / full
	fall	-0.57	-1.22	0.37	0.23	full / oro + therm
142408	spring	-2.66	-2.13	-0.06	-0.90	-
	fall	-4.82	2.61	2.32	-1.00	oro + therm
142409	spring	-1.29	0.67	2.16	0.33	-
142415	fall	-4.26	1.16	0.61	2.63	oro + twind
142417	spring	-0.83	-2.72	3.43	-0.23	-
157895	fall	-0.65	0.88	1.12	0.04	therm / oro
157896	fall	-0.73	0.63	1.48	-0.40	-
157899	fall	-2.10	1.89	6.47	0.47	oro / therm + twind / therm
157900	fall	-0.42	-0.05	2.98	-0.27	null / therm + twind
157902	fall	-1.98	-1.44	7.56	-0.38	oro + therm
157903	fall	-0.74	1.14	0.71	0.59	full
157904	fall	-1.31	3.60	2.55	0.51	oro / oro + therm
157906	fall	-1.16	1.33	4.52	-0.55	twind
mean	spring	-2.10	-0.46	1.81	-0.10	
	fall	-1.83	0.29	2.33	0.35	
sd	spring	1.57	1.64	1.13	1.31	
	fall	1.34	1.72	2.18	0.96	

[a]individual eagles; blank indicates second season for previous ID
[b]posterior means of parameter estimates
[c]model with lowest looic (Vehtari etal., 2016); all models within two looic of the top model listed in order of fit (separated by /); - indicates null did not converge
[d]oro + therm + twind

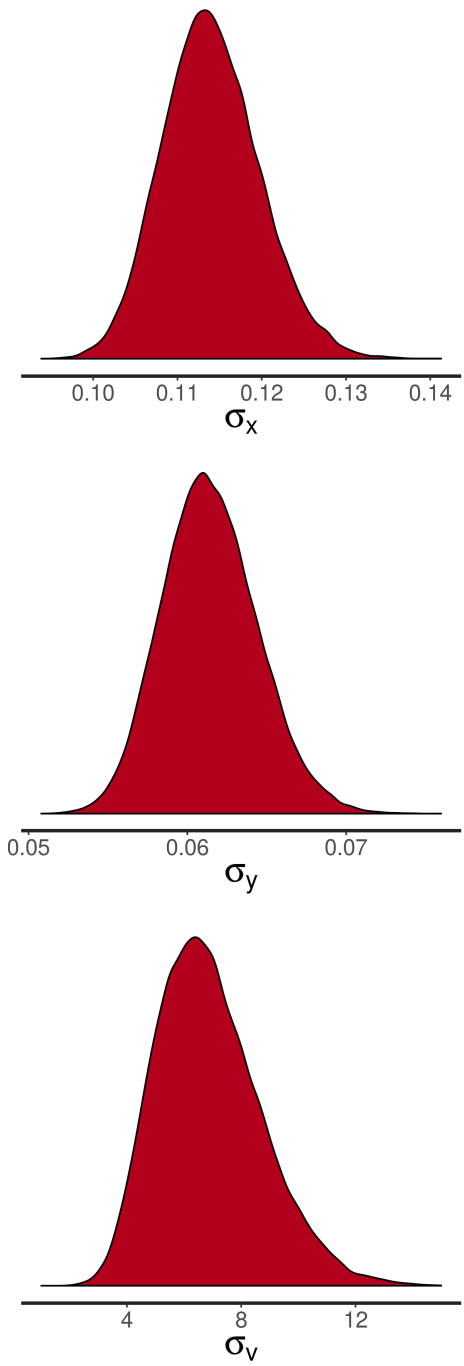

Figure S1: Posterior plots of variance components of the correlated random walk model with orographic uplift, thermal uplift, and tailwind support as behavioral predictors for the spring track of golden eagle 135423. Curves are approximately Gaussian, indicating the model was well behaved and likely converged to the posterior.

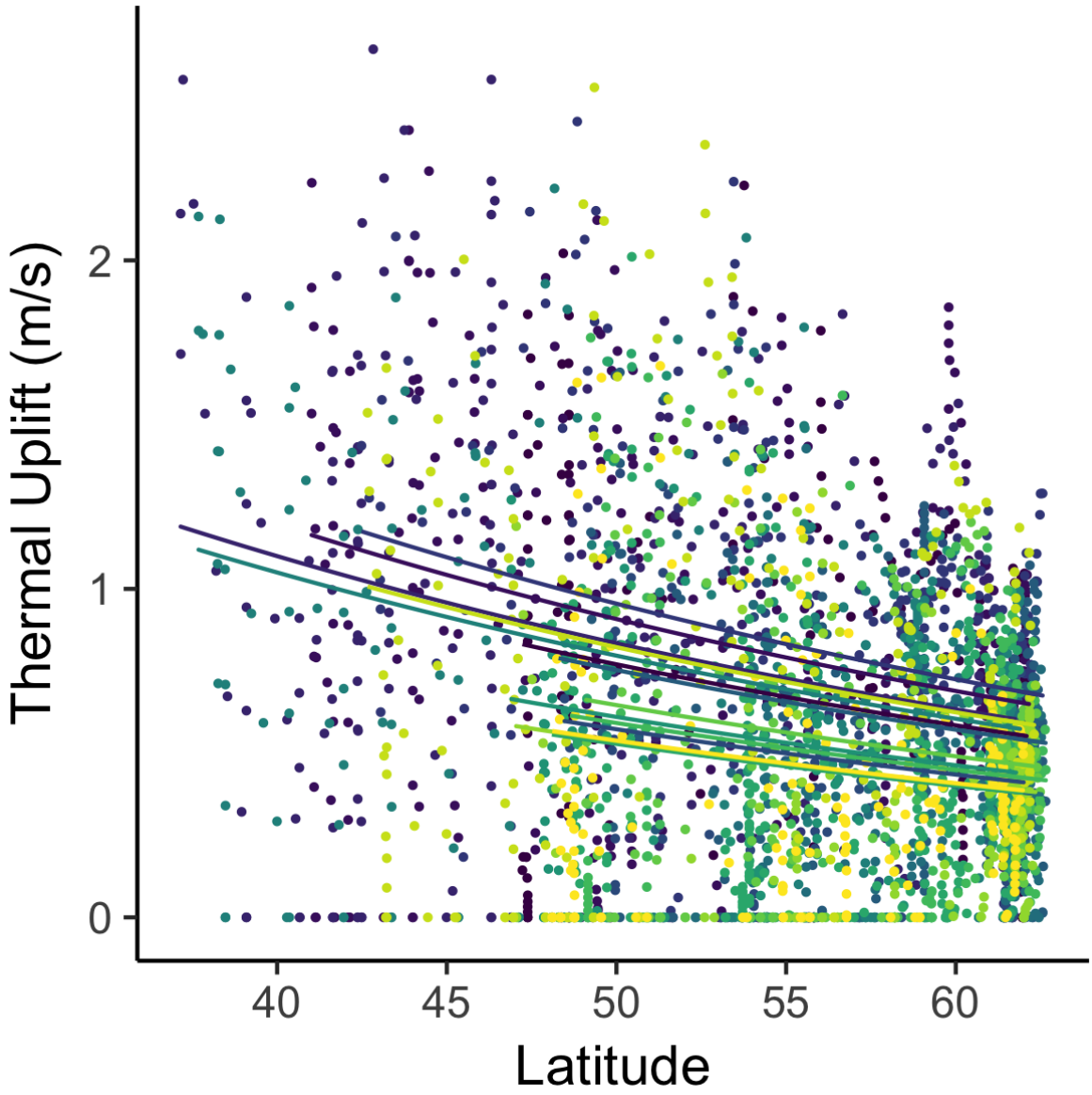

Figure S2: Interpolated thermal uplift as a function of latitude during spring migration. Hue corresponds to individual. Curves are from the individual level of a Bayesian hierarchical Gamma regression. The 95% Bayesian credible interval for the latitude coefficient was $-0.040 < \beta_{lat} < -0.015$, strong evidence for a decreasing trend in thermal uplift with increasing latitude.

Appendix 2: code

Stan model

```
data {

  int N;                // # of fixes in track
  vector[N] x;          // x coordinates
  vector[N] y;          // y coordinates
  vector[N] dt;         // time intervals

  vector[N] oro;        // covariates
  vector[N] therm;
  vector[N] twind;
  vector[N] tod;

}

transformed data {

  vector[N] c_oro;
  vector[N] c_therm;
  vector[N] c_twind;
  vector[N] oro_inter;
  vector[N] therm_inter;
  vector[N] twind_inter;

  // shifted log transform and standardize
  c_oro = ( log( oro + 1 ) * ( 0.5 / sd( log( oro + 1 ) ) ) );

  c_therm = ( log( therm + 1 ) * ( 0.5 / sd( log( therm + 1 ) ) ) );
```

```
  // center and standardize twind
  c_twind = ( ( twind  ) * ( 0.5 / sd( twind ) ) )
  - mean( twind * ( 0.5 / sd( twind ) ) );

  // interactions
  oro_inter = c_oro .* tod;
  therm_inter = c_therm .* tod;
  twind_inter = c_twind .* tod;

}

parameters {

  vector[N] gamma_raw;                // logit behavior parameter
                                      //-- time-varying, correlates steps
  real<lower=0> sigmax;               // variance in x
  real<lower=0> sigmay;               // variance in y
  real<lower=0> sigmav;               // behavior variance
  vector[4] beta;                     // covariate coefficients

}

transformed parameters{

  // introduce logit link
  vector<lower=0,upper=1>[N] gamma;

  for(j in 1:N){
```

```
    gamma[j] = inv_logit( gamma_raw[j] );
  }

}

model {

  // NOTE: Stan uses st. dev. for normals, whereas JAGS uses precision
  // Stan also truncates appropriately based on specified constraints

  // prior on behavior process noise
  // prior density away from zero--assume there is variability in behavior
  sigmav ~ normal( 3 , 3 );

  // priors on movement process noise--close to zero
  sigmax ~ normal( 0 , 1 );
  sigmay ~ normal( 0 , 1 );

  // priors on coefficients
  // prior density on zero--assume no effect of covariates on behavior
  beta ~ student_t( 5, 0 , 2.5 );

  for (i in 3:N) {

    // behavior linear combination of covariates plus previous behavior
    // this can be modified to make candidate formulations
    gamma_raw[i] ~ normal( gamma_raw[i-1] + beta[1]
    + beta[2] * oro_inter[i] + beta[3] * therm_inter[i]
    + beta[4] * twind_inter[i] , dt[i] * sigmav );
```

```
    // movement process is independent in x and y
    x[i] ~ normal( x[i-1] + gamma[i] * ( dt[i] / dt[i-1] )
    * ( x[i-1] - x[i-2] ) , dt[i] * sigmax );

    y[i] ~ normal( y[i-1] + gamma[i] * ( dt[i] / dt[i-1] )
    * ( y[i-1] - y[i-2] ) , dt[i] * sigmay );

  }

}

generated quantities {

  // generate log likelihoods for PSIS-LOO
  // test prediction of next step from previous with estimated gamma
  vector[N] log_lik;
  log_lik[1] = 0.1;  // need something here; simplest to fix across tracks
  log_lik[2] = 0.1;

  for (n in 3:N){

    log_lik[n] = normal_lpdf( x[n] | x[n-1] + gamma[n]
    * ( dt[n] / dt[n-1] ) * ( x[n-1] - x[n-2] ) , dt[n] * sigmax )
    *normal_lpdf( y[n] | y[n-1] + gamma[n] * ( dt[n] / dt[n-1] )
    * ( y[n-1] - y[n-2] ) , dt[n] * sigmay );

  }
```

```

}
```

R code

```
library(rstan)
library(loo)

################################
## model variables
# x -- vector of x coordinates
# y -- vector of y coordinates
# dt -- vector of time intervals
# N -- number of fixes in track
# oro -- vector of raw orographic uplift data
# therm -- vector of raw thermal uplift data
# twind -- vector of raw tailwind data
# tod -- vector of times of day (1=day, 0=night)
################################

dat = read.csv('examp_dat.csv')

x = dat$x
y = dat$y
dt = dat$dt
N = nrow(dat)
oro = dat$oro
therm = dat$therm
twind = dat$twind
tod = dat$tod

# fit Stan model with HMC, using default no-u-turn sampler
# model code should be saved as a .stan file
```

```
# arguments should be modified as required
stan.fit = stan("model.stan",
                data = list(x, y, dt, N, oro, therm, twind, tod),
                chains = 2,
                iter = 1000,
                thin=1,
                cores = 1,
                control = list(adapt_delta = 0.9))
# last argument helps with divergent transitions

# PSIS-LOO
log_lik = extract_log_lik(stan.fit)
loo = loo(log_lik_00)
print(loo)
# use compare(loo1, loo2, ...) to rank candidate models
```